

Conformational Selection and Functional Dynamics of Calmodulin: A ^{19}F Nuclear Magnetic Resonance Study

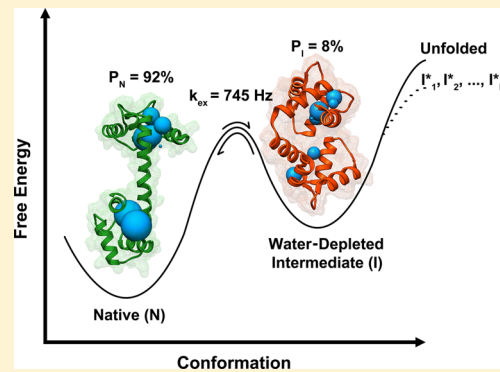
Joshua Hoang[†] and R. Scott Prosser^{*,†,‡}

[†]Department of Chemistry, University of Toronto, UTM, 3359 Mississauga Road North, Mississauga, ON L5L 1C6, Canada

[‡]Department of Biochemistry, University of Toronto, 1 King's College Circle, Toronto, ON M5S 1A8, Canada

Supporting Information

ABSTRACT: Calcium-bound calmodulin (CaM-4Ca²⁺) is innately promiscuous with regard to its protein interaction network within the cell. A key facet of the interaction process involves conformational selection. In the absence of a binding peptide, CaM-4Ca²⁺ adopts an equilibrium between a native state (N) and a weakly populated near-native peptide-bound-like state (I), whose lifetime is on the order of 1.5 ms at 37 °C, based on ^{19}F nuclear magnetic resonance (NMR) Carr–Purcell–Meiboom–Gill (CPMG) relaxation dispersion measurements. This peptide-bound-like state of CaM-4Ca²⁺ is entropically stabilized ($\Delta S = 280 \pm 35 \text{ J mol}^{-1} \text{ K}^{-1}$) relative to the native state, water-depleted, and likely parental to specific bound states. Solvent depletion, conformational selection, and flexibility of the peptide-bound-like state may be important in priming the protein for binding. At higher temperatures, the exchange rate, k_{ex} , appears to markedly slow, suggesting the onset of misfolded or off-pathway states, which retards interconversion between N and I. ^{19}F NMR CPMG relaxation dispersion experiments with both CaM-4Ca²⁺ and the separate N-terminal and C-terminal domains reveal the cooperative role of the two domains in the binding process and the flexibility of the N-terminal domain in facilitating binding. Thus, when calcium binds, calmodulin establishes its interaction with a multitude of protein binding partners, through a combination of conformational selection to a state that is parental to the peptide-bound state and, finally, induced fit.



While proteins are generally recognized to fold in a highly cooperative manner, many exceptions exist, whereby efficient protein folding is achieved via one or more near-native intermediate states.^{1–7} In most cases, the near-native intermediate may be ascribed to a molten globule state, which may be characterized by significant secondary structure, a loss of tight packing between residues associated with the hydrophobic core, an increased hydrodynamic radius, and significant fluctuations in conformation, facilitated in part by side chain disorder.^{8–11} Generally, molten globules are believed to undergo dewetting during folding, whereby the hydrophobic side chains achieve a closer and more restricted association as the protein adopts the compact native state.^{9,12,13} An alternative interpretation of such near-native folding intermediates contends that the molten globule is desolvated or “dry” and is entropically stabilized.^{14–17} However, it is not clear how prevalent the dry molten globule is in proteins known to fold via an intermediate, nor is it clear how dry the desolvated state might be.¹⁸ In this paper, we consider a possible function for a water-depleted intermediate state of calcium-bound calmodulin (CaM-4Ca²⁺) in peptide binding and recognition.

In studying the temperature-dependent folding of CaM-4Ca²⁺, we recently identified a near-native state, which was determined to be reminiscent of a dry molten globule.¹⁹ This state was found to exhibit a higher degree of side chain

disorder, an increased hydrodynamic radius, and decreased access of water to the protein interior, consistent with the description given above.^{15,16} In our case, we prefer the designation of a water-depleted near-native state, because ^{15}N – ^1H and ^{13}C – ^1H nuclear magnetic resonance (NMR) spectra are well-resolved and do not exhibit significant line broadening, characteristic of molten globules and intermediate exchange.¹⁹ Our results made use of ^{19}F NMR solvent isotope shifts, arising from the eight (3-fluoro)phenylalanine residues residing in the protein interior. These isotope shifts showed a pronounced reduction in access of water to the hydrophobic protein interior, while paramagnetic shifts associated with dissolved oxygen revealed a corresponding increase in hydrophobicity.¹⁹ ^{19}F NMR CPMG relaxation dispersion experiments (*vide infra*) show that the native ensemble is transiently populated by this water-depleted near-native state at physiological temperatures. Below, we describe these relaxation dispersion experiments, which reveal millisecond time scale interconversion between the native state and the near-native intermediate.

Received: June 3, 2014

Revised: August 13, 2014

Published: August 22, 2014

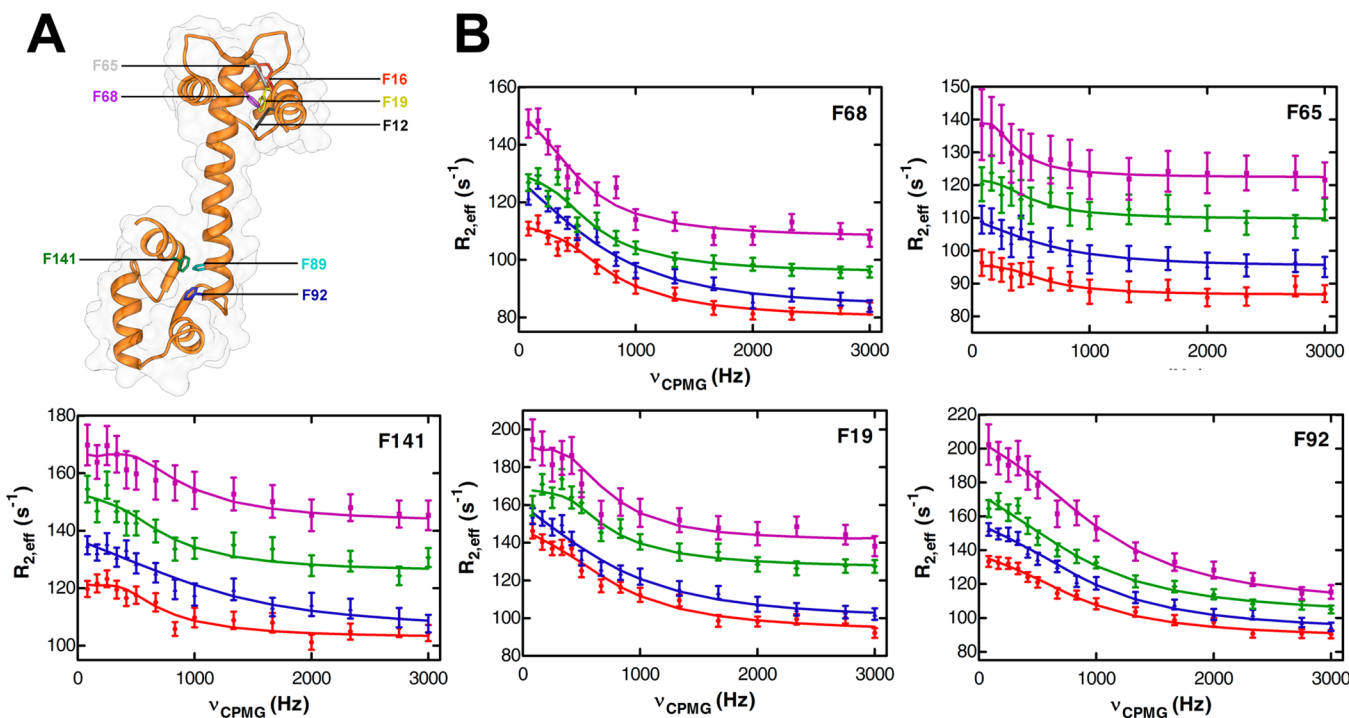


Figure 1. (A) X-ray crystal structure of calcium-loaded calmodulin (Protein Data Bank entry 3CLN) highlighting the position of the eight phenylalanine residues. (B) ^{19}F CPMG relaxation dispersion profiles, obtained at 14.1 T, for five of the eight phenylalanine reporters (F68, F65, F141, F19, and F92) collected at 41 °C (purple), 45 °C (green), 51 °C (blue), and 57 °C (red). Using two field strengths, the dispersion curves were simultaneously fit to a two-site exchange model to extract an exchange rate, k_{ex} . Dispersion profiles for residues F12, F16, and F89, which were not fit because of spectral overlap, are shown in Figure S3 of the Supporting Information.

Very recent work by Clore and co-workers^{20,21} made use of interdomain paramagnetic relaxation effects through the use of a spin-label, to demonstrate that CaM-4Ca²⁺ samples both the native extended (open) state (~90%) and a closed state (~10%) that adopts a peptide-bound topology in the absence of any binding peptide. Because the binding interface of the peptide-bound or “closed” state is too occluded to accommodate the binding peptide without first opening, they reasoned that the peptide-bound state is best represented as a loose and somewhat more disordered ensemble that is primed for peptide binding and accommodates the binding protein through a combination of both conformational selection and induced fit.^{20–27} Our ^{19}F NMR CPMG experiments presented herein identify a similar population of native and near-native states, while also providing a measure of the exchange rates and, therefore, lifetimes associated with each state. We argue that the near-native water-depleted state is indeed the peptide-bound-like state, discussed by Clore and others. Moreover, because the peptide-binding interface of CaM-4Ca²⁺ consists of distinct hydrophobic patches, the transient nature of the peptide-bound-like state likely avoids misfolding, as discussed below. The entropy of the near-native intermediate may also play a role in the kinetics of CaM-4Ca²⁺–peptide binding, much as intrinsically disordered proteins are thought to make use of disorder to sample conformational space and accelerate the protein recognition process.^{28–32} We discuss the possible consequences of a water-depleted near-native state to protein–protein interactions and to misfolding.

MATERIALS AND METHODS

Protein Expression and Purification. Expression and purification of 76% 3-FPhe-labeled CaM-4Ca²⁺ were performed

as previously described.³³ *Xenopus laevis* calmodulin (residues 1–148) was expressed in BL21(DE3) competent cells. Fractional labeling was achieved by supplementing the expression medium with 29.75 g/L 3-fluorophenylalanine and 5.25 g/L DL-phenylalanine at the time of induction. The protein was purified using nickel affinity chromatography followed by phenyl sepharose chromatography. Purified CaM was dialyzed into 20 mM Tris-HCl, 100 mM KCl, 9 mM CaCl₂, and H₂O/D₂O (90:10) buffer adjusted to pH 8.0 and concentrated to 2–3 mM for NMR experiments. An equimolar amount of CaM-dependent protein kinase I (CaMKI, residues 294–318) was added for peptide binding experiments.

Trypsin digestion of full length 3-FPhe CaM-4Ca²⁺ was performed as previously described with several modifications.^{34,35} CaM-4Ca²⁺ (1 mM) was dialyzed into 50 mM NH₄HCO₃, 50 mM NaCl, and 5 mM CaCl₂ buffer adjusted to pH 7.9. CaM-4Ca²⁺ was incubated in the presence of 0.017 M trypsin at 37 °C for 1 h; 0.017 mM soybean trypsin inhibitor was then added to stop the digestion reaction. Using a 50 cm Sephadex G-50 column, the undigested protein was separated from the trypsin fragments by being run through 50 mM NH₄HCO₃, 50 mM NaCl buffer adjusted to pH 7.9. Aliquots containing CaM-4Ca²⁺ trypsin fragments were pooled and separated using a phenyl sepharose column. The C-terminal fragment (TR2C) was first eluted using 2 mM Tris-HCl, 1 mM CaCl₂ buffer adjusted to pH 7.5 followed by elution of the N-terminal fragment (TR1C) using doubly distilled H₂O. TR1C and TR2C were then dialyzed into 20 mM Tris-HCl, 100 mM KCl, 9 mM CaCl₂, and H₂O/D₂O (90:10) buffer adjusted to pH 8.0.

^{19}F CPMG Relaxation Dispersion Experiments. ^{19}F CPMG experiments were conducted at magnetic field strengths

of 11.7 and 14.1 T using a one-dimensional CPMG sequence [i.e., $90^\circ - (\tau_{\text{cp}} - 180^\circ - \tau_{\text{cp}})_N$]. A constant time delay, T_{CPMG} , of 12 ms was used, and a given relaxation series was determined on the basis of spectra resulting from one of 15 values for τ_{CP} [i.e., $\nu_{\text{CPMG}} = 1/(4\tau_{\text{CP}}) = 83, 167, 250, 333, 417, 500, 667, 833, 1000, 1333, 1667, 2000, 2333, 2750, and 3000 s⁻¹]. TR2C CaM-4Ca²⁺ exhibited longer T_2 relaxation times, affording a longer constant time delay. Thus, for the trypsin fragment, TR2C, a T_{CPMG} value of 20 ms was used along with 13 τ_{cp} values ($\nu_{\text{CPMG}} = 50, 100, 150, 200, 300, 500, 700, 900, 1100, 1500, 1900, 2300, \text{ and } 2700 \text{ s}^{-1}$). A T_{CPMG} value of 20 ms and 13 τ_{cp} values ($\nu_{\text{CPMG}} = 50, 100, 150, 200, 250, 350, 450, 650, 850, 1250, 1650, 2050, \text{ and } 2500 \text{ s}^{-1}$) were used for ¹⁹F CPMG experiments on TR1C CaM-4Ca²⁺. The effective transverse relaxation rates [$R_{2,\text{eff}} = (-1/T_{\text{CPMG}}) \times \ln(I/I_0)$] were calculated using extracted intensities, I , where I_0 represents the intensity in the absence of a constant time delay. Errors shown in the dispersion profiles are based on the signal-to-noise ratio of the corresponding spectrum. Relaxation dispersion curves, $R_{2,\text{eff}}$ versus ν_{CPMG} , were fit to a two-state exchange model using ChemEx (<http://code.google.com/p/chemex/>).³⁶ A global fit of dispersions at two field strengths, for residues F68, F65, and F19, was performed to yield an estimate of the populations at 37 °C. Note that relaxation dispersion data at two fields were simultaneously fit to obtain an estimate for the exchange rate, k_{ex} , using completely generalized equations for two-site exchange.³⁷$

¹⁹F T_1 and T_2 Experiments. The measurement of ¹⁹F longitudinal relaxation times (T_1) was accomplished using an inversion recovery sequence ($180^\circ - \tau - 90^\circ$) using a total of 10 τ values, ranging from 1 ms to 0.7 s, and a repetition time of 4 s. For even transients, the $0^\circ - \tau - 90^\circ$ sequence was used and the resulting FIDs were differentiated from those in odd scans. T_1 relaxation times were then calculated by fitting the intensity versus delay time plot to an exponential decay [$I = I_0 \times \exp(-\tau/T_1)$]. ¹⁹F transverse relaxation times (T_2) were calculated by comparing the intensity resulting from the highest refocusing frequency ($\nu_{\text{CPMG}} = 3000 \text{ Hz}$) to that obtained from a simple single excitation pulse. Using the “model-free” approach given by Lipari and Szabo,^{38,39} an order parameter value, S^2 , was determined using T_1 and T_2 relaxation times.

RESULTS

Equilibria with the Water-Depleted Near-Native State.

Figure 1A shows an X-ray structure of CaM-4Ca²⁺, highlighting the positions of the phenylalanine residues, while Figure S1A of the Supporting Information shows a representative ¹⁹F NMR spectrum of 3-FPhe-enriched CaM-4Ca²⁺, with accompanying assignments. The peaks, which are well dispersed, reflect both local secondary structure and subtle differences in packing and the tertiary environment. By monitoring the chemical shift of each residue as a function of temperature, we noted a distinct nonlinear dependence of chemical shift, allowing the determination of the transition temperature and equilibrium between the native state, N, and near-native state, I.¹⁹ This near-native state was characterized as having a less compact protein interior, though its water accessibility was reduced.¹⁹ ¹⁹F NMR proved to be key in identifying the near-native state, both because of the relative sensitivity of the ¹⁹F NMR chemical shift to van der Waals and electrostatic environments and because the ¹⁹F nuclei could be incorporated into the protein interior, without unduly perturbing the protein. At

higher temperatures, though well below the unfolding temperature of ~115 °C,⁴⁰ the equilibrium favors the near-native state, which is found to represent roughly half of the conformational ensemble at 65 °C, based upon chemical shift analysis.¹⁹

The equilibrium between the native (N) and near-native (I) states described above may be corroborated by CPMG relaxation dispersion experiments, which provide an estimate of the relative difference in chemical shifts between two states, their exchange rates, and their relative populations, assuming the states interconvert on a millisecond time scale.^{41,42} A two-field analysis of ¹⁹F NMR CPMG relaxation dispersion profiles, shown in Figure S2 of the Supporting Information, reveals that I represents 8% of the ensemble at 37 °C, suggesting that the near-native state plays a role at physiological temperatures. As discussed below, I may readily undergo interconversion between both the native state and other states, which likely include unfolded (U) and possible off-pathway states (I^{*}₁, I^{*}₂, ..., I^{*}_N).^{43,44}

CPMG Relaxation Dispersion Measurements and Exchange between Native and Non-Native States. If exchange occurs on a T_2 time scale, it is possible to make use of the so-called relaxation-compensated CPMG experiment to determine the relative population, the exchange rate, k_{ex} , and the frequency separation, $\Delta\omega$, between the two states.^{45–47} ¹⁹F NMR CPMG relaxation dispersions provide clear evidence of exchange between the native and near-native states, as shown in Figure 1B and Figures S2 and S3 of the Supporting Information. A key control involved the addition of 5% trifluoroethanol (TFE), which was shown to fully stabilize the native state and abolish any relaxation dispersion or evidence of exchange (Figure S4 of the Supporting Information). With the exception of CPMG studies of apoCaM,^{48–50} nonvertebrate CaM,⁵¹ or CaM mutants,⁵² no prior observations of millisecond time scale exchange by CPMG measurements of CaM-4Ca²⁺, in the absence of other ligands, have been reported. Furthermore, ¹⁵N CPMG relaxation dispersion experiments with ¹⁹F-labeled CaM-4Ca²⁺ did not reveal any dispersions. This speaks to the sensitivity of the ¹⁹F NMR shift to the detection of subtle changes in the environment and to the potential for ¹⁹F NMR CPMG studies of conformational exchange. All of the phenylalanine reporters exhibit a significant relaxation dispersion suggesting that the exchange between N and I represents a global process. However, because of overlap of certain resonances, dispersion profiles from only five residues (F141, F68, F65, F19, and F92) were used to estimate the N–I exchange rate, k_{ex} . A careful examination of the relaxation dispersion profile as a function of temperature shows that the average exchange rate extends from an intermediate time scale at lower temperatures, where a characteristic low-frequency plateau in the dispersions is evident, to a relatively fast time scale at higher temperatures, whereupon the exchange rate decreases upon heating (Figure S5 and Table S1 of the Supporting Information).

The temperature dependence of the exchange rate, as measured by ¹⁹F NMR CPMG relaxation dispersion experiments, is intriguing as it hints at the possibility of additional off-pathway states. Using previous estimates of the native and near-native state populations, p_N and p_I , respectively, based on chemical shifts, it is possible to calculate both folding (k_{IN}) and unfolding rates (k_{NI}), given that $k_{\text{ex}} = k_{\text{IN}}/p_N = k_{\text{NI}}/p_I$, as a function of temperature (Figure 2A and Table S1 of the Supporting Information). As shown in Figure 2A, the folding rate increases with temperature, until reaching 51 °C

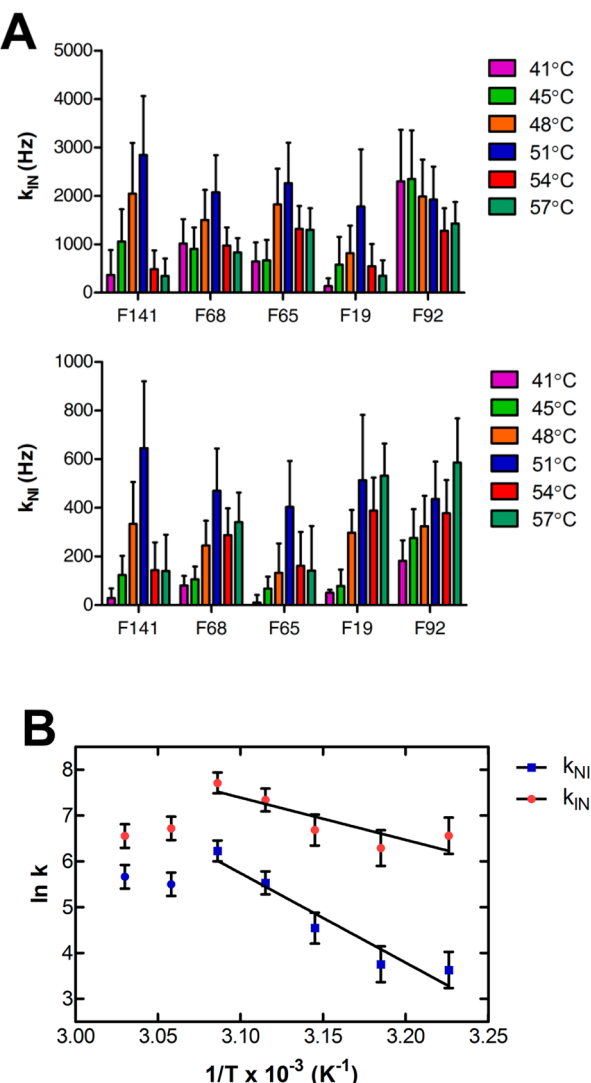


Figure 2. (A) Folding, k_{IN} (top), and unfolding, k_{NI} (bottom), rates as a function of temperature. (B) Arrhenius plot of folding and unfolding rates, averaged for residues F141, F68, F65, and F19. An Arrhenius analysis reveals activation energies of 77 ± 25 and 163 ± 27 kJ/mol for the folding and unfolding processes, respectively. Because of the non-Arrhenius behavior of the exchange rates at higher temperatures, exchange rates measured at 54 and 57 °C were omitted from the activation energy analysis.

whereupon it appears to decrease precipitously above this temperature. The one exception is F92, which exhibits significant exchange, albeit with a different temperature-dependent profile. The resonance at F92 can at some temperatures be observed to display a small shoulder. Thus, there may be additional processes taking place, associated with F92, which cannot be described by a two-state exchange model. Between 37 and 51 °C, the unfolding rate also increases with temperature, even more steeply than that of the folding rate. An Arrhenius analysis (Figure 2B) of the temperature dependence of the folding and unfolding rates suggests that the activation energies associated with the partial folding and unfolding processes are 77 ± 25 and 163 ± 27 kJ/mol, respectively. The abrupt decrease in folding and unfolding rates above 51 °C is consistent with a model in which additional off-pathway states ($I^*_{1, 2, \dots, N}$, and U) become accessible at higher temperatures. Prior single-molecule experiments with CaM-

$4Ca^{2+}$ reveal a complex folding network, consisting of multiple on- and off-pathway folding intermediates.^{43,44,53,54} Rief et al. showed evidence of EF hand exchange and off-pathway (entangled) states associated with CaM-4Ca²⁺.^{43,44,53} These authors noted that while the individual domains of CaM-4Ca²⁺ can fold within microseconds, complete folding of CaM-4Ca²⁺ has a long average folding time because of the presence of off-pathway intermediates.⁴⁴ Thus, at higher temperatures, it is possible that these so-called off-pathway states are accessed, in which case, reversion to a disentangled state would be necessary before the N and I states can exchange.

The Water-Depleted Near-Native State and Entropy Considerations.

One signature of the dry molten globule state is that it is stabilized both by system entropy, through the expulsion of water, and by configurational entropy, as exhibited by large-amplitude side chain fluctuations and less compact states.⁵⁵ We regard the near-native state of CaM-4Ca²⁺ as water-depleted and similarly disordered, though to a lesser extent than that expected for a molten globule, given the observed amide ¹H chemical shift dispersions at temperatures at which the near-native state dominates. To some extent, we can assess the configurational entropy of CaM-4Ca²⁺ by an order parameter analysis. This is most easily achieved through a Lipari-Szabo model-free analysis of T_1 and T_2 relaxation times, which characterizes faster side chain motions and, in particular, configurational entropy.^{38,39,56}

An orientational order parameter, S^2 , and an internal correlation time, τ_i , can be obtained from an analysis of T_1 and T_2 relaxation times and used to describe the respective amplitude and time scale of local reorientation for a given side chain. The order parameter ranges from 1, for a restricted motion, to 0, for a more flexible motion. The order parameters for five of the eight fluorophenylalanine reporters display a clear trend with temperature as depicted in Figure S1B of the Supporting Information and compare favorably to those previously measured for methionine residues in CaM-4Ca²⁺.⁵⁶ Elevated temperatures, where the near-native state, I, dominates, result in a marked decrease in order parameter values that range from 0.14 to 0.17 at 57 °C. The lower order parameter values signify loosening of the hydrophobic core whereupon the amplitudes of side chain motions increase and the configurational entropy of the protein is characteristically high.

It is also possible to examine the thermodynamic driving forces toward the formation of the water-depleted near-native state. If we focus on temperatures in the vicinity of the transition to the near-native state (45–70 °C), it is possible to estimate the enthalpy and entropy changes (i.e., ΔH_{NI} and ΔS_{NI} , respectively) the system undergoes upon converting from the native, N, to water-depleted near-native state, I, where

$$\ln K_{NI} = -\Delta H_{NI}/RT + \Delta S_{NI}/R \quad (1)$$

Note that this analysis assumes that the state specific enthalpies are constant over the temperature range studied and that the equilibrium is strictly associated with the two states mentioned above. By making use of the N–I equilibrium data, based on prior ¹⁹F NMR chemical shift analyses, and assuming the equilibrium constant is equal to the ratio of the populations of the two states, we estimate the enthalpy and entropy changes to be 94 ± 12 kJ/mol and 280 ± 35 J mol⁻¹ K⁻¹, respectively (Figure S6 of the Supporting Information). Thus, the near-native intermediate is strongly entropically stabilized and likely arises due to both configurational entropy (side chain disorder)

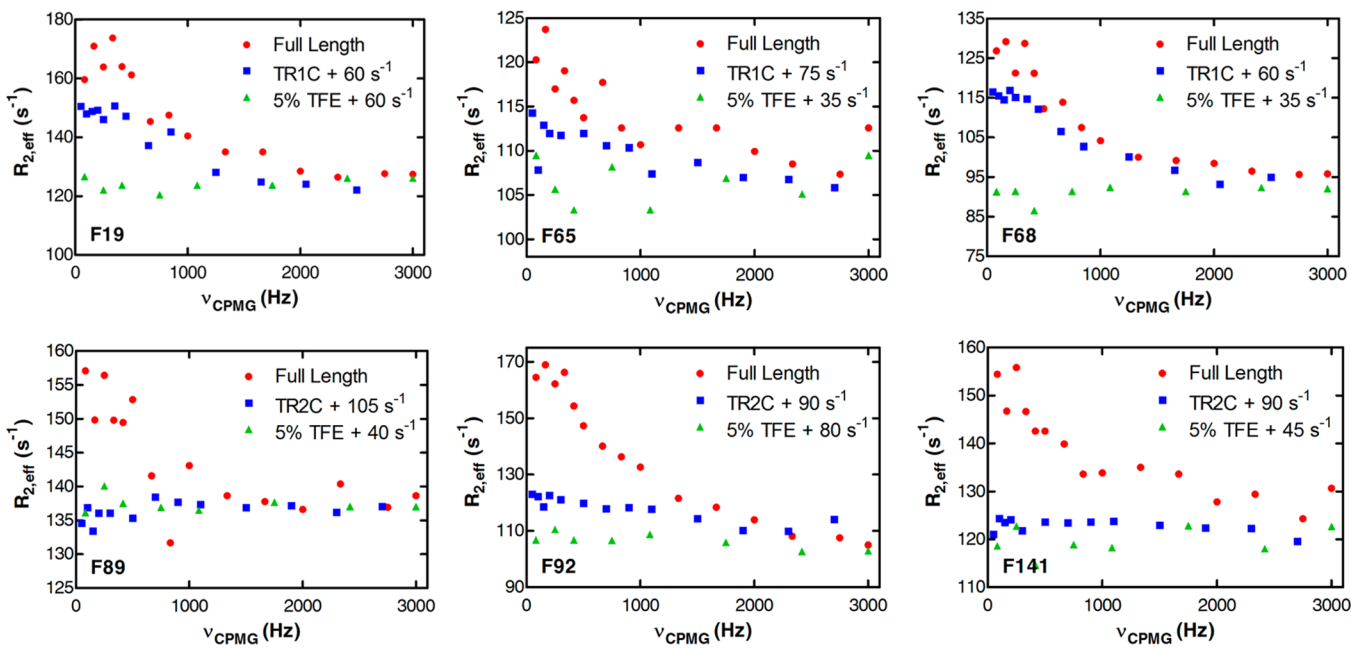


Figure 3. ^{19}F CPMG relaxation dispersion profiles for full length CaM-4Ca $^{2+}$ (red), TR1C (blue, top trace), and TR2C (blue, bottom trace) at 45 °C. The CPMG dispersion from full length CaM-4Ca $^{2+}$ in the presence of 5% TFE (green) is shown as a control to indicate the absence of exchange. As shown in the figure legend, a constant value was added to $R_{2,\text{eff}}$ values for the dispersion curves of TR1C, TR2C, and 5% TFE to make a comparison to the full length CPMG dispersions. The raw CPMG dispersion data for all curves are shown in Table S2 of the Supporting Information.

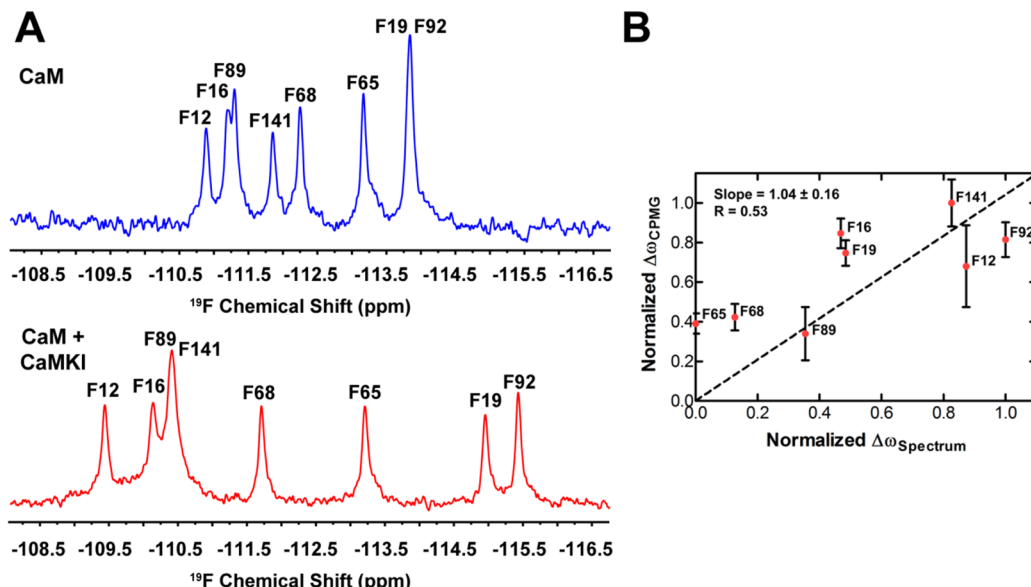


Figure 4. (A) ^{19}F spectra of CaM-4Ca $^{2+}$ in the presence (red) and absence (blue) of the binding peptide, CaMKI (residues 294–318), at 41 °C. Peak assignments of the peptide-bound state are tentative and are based on the assumption that the peaks remain in the same order as those in the peptide-free state. (B) Correlation plot showing the relationship between $\Delta\omega_{\text{CPMG}}$ and $\Delta\omega_{\text{spectrum}}$.

and the liberation of waters. We note that on a per residue basis, these values are remarkably similar to the measured changes associated with the unlocking of a villin headpiece subdomain, which was purported to adopt a dry molten globule state.⁵⁷

Cooperativity between the N- and C-Terminal Domains and the Connection to the Peptide-Bound State. To investigate the potential role of cooperativity between the N-terminal and C-terminal domains in folding, we repeated the ^{19}F NMR spectroscopy and CPMG relaxation

dispersion experiments on the separate N- and C-terminal domains. The N- and C-terminal domains (denoted TR1C and TR2C, respectively) can be obtained through a trypsin digest of full length CaM-4Ca $^{2+}$. Figure 3 compares ^{19}F NMR CPMG relaxation dispersion profiles of full length CaM-4Ca $^{2+}$ and those of TR1C and TR2C at 45 °C. A relaxation dispersion profile of full length CaM-4Ca $^{2+}$ with 5% TFE is also included as a control to show that no exchange is present upon stabilization of the native state.¹⁹ As indicated by the CPMG dispersion profiles, it is immediately clear that exchange

dynamics differ significantly between full length CaM-4Ca²⁺ and its isolated N- and C-terminal domains. This result suggests that exchange processes monitored in full length CaM-4Ca²⁺ arise partly from transient interactions between the N- and C-terminal domains, as suggested previously.⁵⁸ Note from Figure 3 that little or no exchange is observed for TR2C alone.⁵⁹ This is corroborated by recent molecular dynamics simulations in that the isolated N-terminal domain of CaM-4Ca²⁺ is observed to be inherently more flexible than the isolated C-terminal domain.^{60,61} Such flexibility may facilitate interconversion between different states on a millisecond time scale for the N-terminal domain alone. Thus, exchange measured in full length CaM-4Ca²⁺ is partly a result of a transient interaction between two domains and is driven by the inherent flexibility of the N-terminal domain. This result might appear to be in conflict with previously detailed NMR relaxation studies of CaM-4Ca²⁺, which revealed that the C-terminal domain is in fact slightly more disordered than the N-terminal domain in the sense that it exhibits marginally lower backbone order parameters.⁵⁹ However, the order parameter, which is a measure of the amplitude of local backbone reorientations on a picosecond time scale, likely does not capture millisecond time scale interconversions between N and I, which we associate with conformational flexibility.

The striking difference in relaxation dispersion behavior between the N- and C-terminal domains led us to consider the possibility that the water-depleted near-native state, I, is best approximated as a peptide-bound conformation, because the N- and C-terminal domains are known to behave differently during peptide binding.⁶² Furthermore, there is compelling evidence that the peptide-bound state is sampled in the absence of peptide.^{7,20} In particular, previous experiments that made use of (long-range) paramagnetic relaxation effects from a spin-label introduced via a single-cysteine point mutation identified a compact state, which resembled a peptide-bound state and was believed to prime calmodulin for binding.²⁰ Figure 4A compares the ¹⁹F NMR spectra between CaM-4Ca²⁺ in the absence and presence of a binding peptide (CaMKI, residues 294–318), from which we may estimate the frequency separation, $\Delta\omega_{\text{spectrum}}$ ($=2\pi\Delta\nu$), between the free and peptide-bound state, for each residue. If exchange to a peptide-bound state occurs on a T_2 time scale, we expect that the fitted residue specific frequency separation from the CPMG dispersions, $\Delta\omega_{\text{CPMG}}$, will approximate the spectroscopically obtained frequency differences described above, barring gross chemical shift perturbations that would result if the ¹⁹F nuclei were in the proximity of the binding peptide. Note that the frequency separation, excited state population, and exchange rate, k_{ex} , are all determined by simultaneously fitting the observed ¹⁹F NMR relaxation dispersion profiles obtained at two field strengths, as described in Materials and Methods.

We emphasize that CaM-4Ca²⁺ is known to bind to a large family of proteins, so that there is significant variability expected in the peptide-bound conformation.^{23,63} Thus, rather than a distinct bound conformation, we expect that the peptide-bound-like state is best represented by an ensemble of rapidly interconverting conformers, which approximate a peptide-bound state and prime the protein for binding.²⁰ Furthermore, the peptide-bound state, sampled in the absence of binding peptide, must clearly be more open to facilitate entry of binding peptide. We therefore regard the peptide-bound-like state as “parental” to the specific peptide-bound states, achieved only through binding. Nevertheless, a reasonable correlation is

observed between $\Delta\omega_{\text{CPMG}}$ and the frequency separations derived from the spectrum, $\Delta\omega_{\text{spectrum}}$, for a single representative binding peptide, CaMKI(294–318), as shown in Figure 4B. We conclude that the CPMG dispersion arises from two-site exchange between the peptide-free (native) state, N, and a state that may be described as peptide-bound-like (I). Using spin-labels and interdomain relaxation effects, Anthis and co-workers reached the same conclusion, namely, that CaM-4Ca²⁺ samples a “closed” or peptide-bound-like state.^{20,24} Moreover, the relative population of the peptide-bound ensemble was within error identical to our estimate of 8% at physiological temperatures. Finally, binding of the peptide, CaMKI, which is known to establish a well-defined “closed state” of CaM-4Ca²⁺, abolishes the exchange process and, thus, all CPMG dispersions, with the exception of F92 that exhibits a weak dispersion.

■ DISCUSSION

The Near-Native Ensemble and Consequences of Peptide Binding. Protein–protein and protein–ligand interactions are thought to take place through a combination of conformational selection and induced fit. The extent to which one mechanism dominates over the other in a given interaction generally depends on the system and the relative concentration of the ligand or binding partner.⁶⁴ Binding of peptide to CaM-4Ca²⁺ is recognized to involve partial unwinding of the central flexible linking helix and a subtle shift in interhelical angles within the N- and C-terminal domains, thereby exposing methionine-rich hydrophobic patches, which primes the protein for binding.^{65–67} CaM-4Ca²⁺ is known to bind to literally hundreds of proteins and, in particular, a wide variety of serine/threonine kinases, including CaM kinase I and II, CaM-kinase kinase, and myosin light chain kinases.^{22,23} This begs the question of how such promiscuous proteins might accomplish binding in terms of the mechanisms mentioned above. If conformational selection represents a dominant mechanism through which CaM-4Ca²⁺ interacts with its binding partners, then the representative “bound” conformations must all be frequently sampled. Moreover, we would also expect that promiscuous binding proteins such as CaM-4Ca²⁺ would exhibit greater flexibility to accomplish this task, as has been suggested by others.^{20,21,62,68–70} Thus, as proposed in the introductory section, we conclude that the peptide-bound-like state is best represented as a loose and somewhat more disordered ensemble that is primed for peptide binding and accommodates the binding protein through a combination of both conformational selection and induced fit.^{20–27} The role of the binding peptide in achieving specificity through mutually induced conformational changes has also been discussed recently.⁶²

The description given above of the peptide-bound state in terms of a loose ensemble is also consistent with our NMR studies, which determined that the near-native state is entropically stabilized and exhibits an increased level of configurational disorder.¹⁹ A high level of disorder of the near-native peptide-bound-like state is also a distinct advantage because the protein would be expected to accommodate binding peptides of varying sequence and structure through induced fit. Intrinsically disordered proteins are suggested to undergo a kind of presampling over significant conformational space,⁷¹ though the peptide-bound-like state is clearly a less extreme example of a true intrinsically disordered protein.^{31,71–74} Disordered proteins also often undergo a disorder

to order transition upon binding, which has been shown to result in a reduced binding free energy barrier, thereby facilitating faster kinetics.⁷⁵ Similarly, formation of the peptide-bound-like state, I, is strongly entropically driven ($\Delta S = 280 \pm 35 \text{ J mol}^{-1} \text{ K}^{-1}$), and the “disorder to order” scenario depicted above for binding seems reasonable for a protein such as CaM-4Ca²⁺, which in the peptide-bound-like state must accommodate a wide range of binding partners.

Role of the Water-Depleted Near-Native State. Protein folding is typically described as an entropically driven process in which the unfolded protein undergoes hydrophobic collapse, thereby liberating water molecules in the process. Here, we observe a surprising exception to the rule in that the peptide-bound-like state is water-depleted and is in fact entropically stabilized over the native state, both because of the release of water molecules and because of configurational disorder. The results are reminiscent of previous descriptions of dry molten globule states,^{15,16} with the exception that the near-native state in this case possesses significant secondary and tertiary structure, as evidenced by ¹⁵N-¹H HSQC spectra. We can also not definitively claim whether the near-native state is involved in protein folding. However, a more interesting notion is the possibility that the water-depleted near-native state plays a functional role in peptide binding. While much has been written about the role of conformational selection in protein binding interactions, this is a particularly intriguing example in that the presampled state is relatively disordered and water-depleted. The majority of kinases, known to interact with CaM-4Ca²⁺, exhibit a motif that is largely helical and consists of hydrophobic patches, and specific basic regions, flanked by aromatics.²³ Thus, depletion water, at least in the vicinity of the phenylalanine residues in CaM-4Ca²⁺, likely greatly facilitates the binding process. This is reminiscent of the work of Lawrence et al. that describes an intrinsically disordered protein whose binding to a protein target relieves frustrations associated with a hydrophobic interface, establishing a stable globular complex, in analogy with protein folding.⁷⁶ Here, we describe a water-depleted near-native excited state that may either “fold”, adopting the native state, or bind to a peptide binding partner, similarly relieving this hydrophobic frustration.

One potential drawback of a water-depleted state involves stability, because exposed hydrophobic patches would be expected to leave the protein susceptible to misfolding. CPMG studies, discussed above, reveal that the lifetime of the near-native peptide-bound like state is 1.5 ms at 37 °C (Figure 5). This lifetime may be ideal for CaM-4Ca²⁺ to engage in binding to a target peptide, in contrast to a persistent but weakly populated near-native state that might succumb to misfolding.⁴⁴

Cooperativity in Binding. The surprising difference between ¹⁹F NMR CPMG relaxation dispersions for full length CaM-4Ca²⁺ and the separate TR1C (N-terminal domain) and TR2C (C-terminal domain) species in many ways supports current ideas regarding peptide binding. In particular, recent molecular dynamics studies show that the N-terminal domain of CaM-4Ca²⁺ is inherently more flexible while the C-terminal domain exhibits a higher affinity for most CaM-4Ca²⁺ targets.^{60,61} The residual CPMG dispersions observed with TR1C illustrate the relative conformational flexibility exhibited by the N-terminal domain from the perspective of both sampling states and binding. The significant enhancement of dispersions for full length CaM-4Ca²⁺ also implies some level of cooperativity in the overall exchange process between the

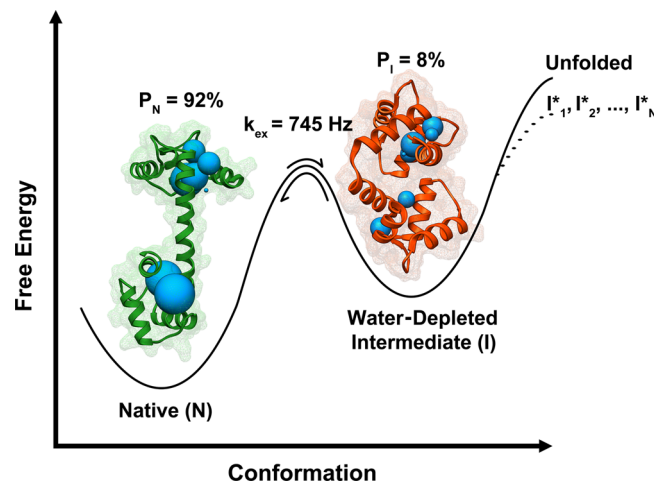


Figure 5. Schematic illustrating the equilibrium between the native state (N, Protein Data Bank entry 3CLN) and the water-depleted intermediate (I). Water accessibility, as measured by previous ¹⁹F NMR solvent isotope shifts, is depicted by the blue spheres. ¹⁹F CPMG experiments reveal that N and I exchange at a rate of $745 \pm 190 \text{ Hz}$ and that the I state represents 8% of the ensemble at 37 °C. In addition to the pathway to the unfolded state (U), the dotted line denotes an alternate folding-unfolding pathway that leads to possible off-pathway intermediate states ($I^*_1, I^*_2, \dots, I^*_N$). Note that in the absence of an experimentally derived structure, the intermediate state is represented by a known peptide-bound state (Protein Data Bank entry 1MXE). We emphasize that our model depicts the peptide-bound-like state as being highly dynamic and more open, likely through the hinge region, such that a binding peptide could be accommodated as discussed in the text.

native and peptide-bound states. Given the difference in dispersion profiles, it is likely that conformational selection is achieved cooperatively as both the C- and N-terminal domains convert from the native to the peptide-bound state, while the N-terminal domain may in some cases be responsible for accommodating the specific binding protein once the interaction is initiated through the C-terminal domain.

CONCLUSIONS

Formerly, we determined that CaM-4Ca²⁺ adopts an equilibrium between a native state and a near-native water-depleted state.¹⁹ We can now conclude that the near-native state is in fact a peptide-bound-like state, thus representing an example in which conformational sampling plays a key role in the binding process. The CPMG relaxation dispersion experiments on the separate N- and C-terminal domains also suggest a cooperative role for both domains in the binding process in which the final complex may in fact be negotiated largely by the N-terminal domain through an induced fit mechanism.

The near-native (peptide-bound-like) state in this case is somewhat exceptional in that it is water-depleted, at least in the vicinity of the phenylalanine residues. Water depletion and intrinsic disorder in the peptide-bound-like state both represent aspects that are advantageous to the binding process. Finally, on the basis of observations that the near-native state has a much higher entropy, peptide binding may represent an example of a disorder to order transition. This situation has distinct advantages with respect to the kinetics and efficiency of the binding process, particularly where there may be many protein-binding partners.

ASSOCIATED CONTENT

Supporting Information

¹⁹F NMR spectrum of 3-FPhe fractionally labeled calcium-bound CaM at 51 °C with the corresponding assignments and order parameters (Figure S1), ¹⁹F CPMG relaxation dispersion profiles at 37 °C (Figure S2), ¹⁹F CPMG relaxation dispersion profiles at 45 °C with fits using data from two field strengths of 11.7 T (blue) and 14.1 T (green) (Figure S3), ¹⁹F CPMG relaxation dispersion profiles for additional residues not shown in the main body of the paper (Figure S4), ¹⁹F CPMG relaxation dispersion profiles for full length CaM-4Ca²⁺ in the presence of 5% trifluoroethanol at 57 °C (Figure S5), exchange rates (k_{ex}), extracted from the CPMG experiments, as a function of temperature (Figure S6), a van't Hoff analysis associated with the formation of the water-depleted intermediate state (Figure S7), exchange (k_{ex}), folding (k_{IN}), and unfolding (k_{NI}) rates extracted from CPMG dispersion experiments for the phenylalanine residues (Table S1), and CPMG relaxation dispersion data ($R_{2\text{eff}}$ vs ν_{CPMG}) for full length CaM-4Ca²⁺, TR1C, TR2C, and full length CaM-4Ca²⁺ in the presence of 5% TFE at 45 °C (Table S2). This material is available free of charge via the Internet at <http://pubs.acs.org>.

AUTHOR INFORMATION

Corresponding Author

*Department of Chemistry, University of Toronto, UTM, 3359 Mississauga Rd. N., Mississauga, ON L5L 1C6, Canada. E-mail: scott.prosser@utoronto.ca. Phone: (905) 828-3802.

Funding

Supported by a NSERC research discovery award (Grant 261980).

Notes

The authors declare no competing financial interest.

ACKNOWLEDGMENTS

We are grateful to comments and advice from Prof. Lewis Kay, Mitsu Ikura, and Julie Forman-Kay, all at the University of Toronto. We also thank William Thach for assisting with CPMG experiments and Rohan Alvares for help with the peptide binding experiments.

ABBREVIATIONS

3-FPhe, 3-fluorophenylalanine; CaM, calmodulin; CPMG, Carr-Purcell-Meiboom-Gill; HSQC, heteronuclear single-quantum coherence.

REFERENCES

- Brockwell, D. J., and Radford, S. E. (2007) Intermediates: Ubiquitous species on folding energy landscapes? *Curr. Opin. Struct. Biol.* 17, 30–37.
- Dill, K. A., Bromberg, S., Yue, K. Z., Fiebig, K. M., Yee, D. P., Thomas, P. D., and Chan, H. S. (1995) Principles of Protein Folding: A perspective from simple exact models. *Protein Sci.* 4, 561–602.
- Kim, P. S., and Baldwin, R. L. (1990) Intermediates in the folding reactions of small proteins. *Annu. Rev. Biochem.* 59, 631–660.
- Onuchic, J. N., LutheySchulten, Z., and Wolynes, P. G. (1997) Theory of protein folding: The energy landscape perspective. *Annu. Rev. Phys. Chem.* 48, 545–600.
- Roder, H., and Colon, W. (1997) Kinetic role of early intermediates in protein folding. *Curr. Opin. Struct. Biol.* 7, 15–28.
- Slaughter, B. D., Unruh, J. R., Price, E. S., Huynh, J. L., Urbauer, R. J. B., and Johnson, C. K. (2005) Sampling unfolding intermediates in calmodulin by single-molecule spectroscopy. *J. Am. Chem. Soc.* 127, 12107–12114.
- (7) Yamada, Y., Matsuo, T., Iwamoto, H., and Yagi, N. (2012) A Compact Intermediate State of Calmodulin in the Process of Target Binding. *Biochemistry* 51, 3963–3970.
- (8) Dolgikh, D. A., Gilmanishin, R. I., Brazhnikov, E. V., Bychkova, V. E., Semisotnov, G. V., Venyaminov, S. Y., and Ptitsyn, O. B. (1981) α -Lactalbumin: Compact state with fluctuating tertiary structure. *FEBS Lett.* 136, 311–315.
- (9) Arai, M., and Kuwajima, K. (2000) Role of the molten globule state in protein folding. *Adv. Protein Chem.* 53, 209–282.
- (10) Naganathan, A. N., and Orozco, M. (2011) The Native Ensemble and Folding of a Protein Molten-Globule: Functional Consequence of Downhill Folding. *J. Am. Chem. Soc.* 133, 12154–12161.
- (11) Uversky, V. N. (2013) Under-folded proteins: Conformational ensembles and their roles in protein folding, function, and pathogenesis. *Biopolymers* 99, 870–887.
- (12) Dyson, H. J., and Wright, P. E. (2004) Unfolded proteins and protein folding studied by NMR. *Chem. Rev.* 104, 3607–3622.
- (13) Mittermaier, A., Korzhnev, D. M., and Kay, L. E. (2005) Side-chain interactions in the folding pathway of a Fyn SH3 domain mutant studied by relaxation dispersion NMR spectroscopy. *Biochemistry* 44, 15430–15436.
- (14) Kieffaber, T., Labhardt, A. M., and Baldwin, R. L. (1995) Direct NMR evidence for an intermediate preceding the rate-limiting step in the unfolding of ribonuclease-A. *Nature* 375, 513–515.
- (15) Jha, S. K., and Udgaonkar, J. B. (2009) Direct evidence for a dry molten globule intermediate during the unfolding of a small protein. *Proc. Natl. Acad. Sci. U.S.A.* 106, 12289–12294.
- (16) Baldwin, R. L., Frieden, C., and Rose, G. D. (2010) Dry molten globule intermediates and the mechanism of protein unfolding. *Proteins: Struct., Funct., Bioinf.* 78, 2725–2737.
- (17) Bhattacharyya, S., and Varadarajan, R. (2013) Packing in molten globules and native states. *Curr. Opin. Struct. Biol.* 23, 11–21.
- (18) Sosnick, T. R., and Barrick, D. (2011) The folding of single domain proteins: Have we reached a consensus? *Curr. Opin. Struct. Biol.* 21, 12–24.
- (19) Kitevski-LeBlanc, J. L., Hoang, J., Thach, W., Larda, S. T., and Prosser, R. S. (2013) F-19 NMR studies of a desolvated near-native protein folding intermediate. *Biochemistry* 52, 5780–5789.
- (20) Anthis, N. J., Doucette, M., and Clore, G. M. (2011) Transient, Sparsely Populated Compact States of Apo and Calcium-Loaded Calmodulin Probed by Paramagnetic Relaxation Enhancement: Interplay of Conformational Selection and Induced Fit. *J. Am. Chem. Soc.* 133, 18966–18974.
- (21) Anthis, N. J., and Clore, G. M. (2013) The Length of the Calmodulin Linker Determines the Extent of Transient Interdomain Association and Target Affinity. *J. Am. Chem. Soc.* 135, 9648–9651.
- (22) Crivici, A., and Ikura, M. (1995) Molecular and Structural Basis of Target Recognition by Calmodulin. *Annu. Rev. Biophys. Biomol. Struct.* 24, 85–116.
- (23) Hoeflich, K. P., and Ikura, M. (2002) Calmodulin in action: Diversity in target recognition and activation mechanisms. *Cell* 108, 739–742.
- (24) Clore, G. M. (2014) Interplay between conformational selection and induced fit in multidomain protein–ligand binding probed by paramagnetic relaxation enhancement. *Biophys. Chem.* 186, 3–12.
- (25) Feixas, F., Lindert, S., Sinko, W., and McCammon, J. A. (2014) Exploring the role of receptor flexibility in structure-based drug discovery. *Biophys. Chem.* 186, 31–45.
- (26) Hatzakis, N. S. (2014) Single molecule insights on conformational selection and induced fit mechanism. *Biophys. Chem.* 186, 46–54.
- (27) Vogt, A. D., Pozzi, N., Chen, Z., and Di Cera, E. (2014) Essential role of conformational selection in ligand binding. *Biophys. Chem.* 186, 13–21.

(28) Wand, A. J. (2013) The dark energy of proteins comes to light: Conformational entropy and its role in protein function revealed by NMR relaxation. *Curr. Opin. Struct. Biol.* 23, 75–81.

(29) Tompa, P. (2002) Intrinsically unstructured proteins. *Trends Biochem. Sci.* 27, 527–533.

(30) Uversky, V. N. (2002) Natively unfolded proteins: A point where biology waits for physics. *Protein Sci.* 11, 739–756.

(31) Dyson, H. J., and Wright, P. E. (2005) Intrinsically unstructured proteins and their functions. *Nat. Rev. Mol. Cell Biol.* 6, 197–208.

(32) Mittag, T., and Forman-Kay, J. D. (2007) Atomic-level characterization of disordered protein ensembles. *Curr. Opin. Struct. Biol.* 17, 3–14.

(33) Kitevski-LeBlanc, J. L., Evanics, F., and Prosser, R. S. (2010) Optimizing F-19 NMR protein spectroscopy by fractional biosynthetic labeling. *J. Biomol. NMR* 48, 113–121.

(34) Kitevski-LeBlanc, J. L., Al-Abdul-Wahid, M. S., and Prosser, R. S. (2009) A mutagenesis-free approach to assignment of F-19 NMR resonances in biosynthetically labeled proteins. *J. Am. Chem. Soc.* 131, 2054–2055.

(35) Brokx, R. D., and Vogel, H. J. (2002) Proteolytic Fragments of Calmodulin-Binding Proteins. In *Calcium-Binding Proteins Protocols*, pp 183–193, Humana Press Inc., Totowa, NJ.

(36) Shi, L. C., and Kay, L. E. (2014) Tracing an allosteric pathway regulating the activity of the HsIV protease. *Proc. Natl. Acad. Sci. U.S.A.* 111, 2140–2145.

(37) Korzhnev, D., and Kay, L. (2008) Probing invisible, low-populated states of protein molecules by relaxation dispersion NMR spectroscopy: An application to protein folding. *Acc. Chem. Res.* 41, 442–451.

(38) Lipari, G., and Szabo, A. (1982) Model-free approach to the interpretation of Nuclear Magnetic Resonance relaxation in macromolecules. 1. Theory and range of validity. *J. Am. Chem. Soc.* 104, 4546–4559.

(39) Lipari, G., and Szabo, A. (1982) Model-free approach to the interpretation of nuclear magnetic resonance relaxation in macromolecules. 2. Analysis of experimental results. *J. Am. Chem. Soc.* 104, 4559–4570.

(40) Shiba, K., Niidome, T., Katoh, E., Xiang, H., Han, L., Mori, T., and Katayama, Y. (2010) Polydispersity as a parameter for indicating the thermal stability of proteins by dynamic light scattering. *Anal. Sci.* 26, 659–663.

(41) Palmer, A. G., Kroenke, C. D., and Loria, J. P. (2001) *Nuclear magnetic resonance methods for quantifying microsecond-to-millisecond motions in biological macromolecules*, Vol. 339, Academic Press, San Diego.

(42) Hansen, D. F., Vallurupalli, P., Lundström, P., Neudecker, P., and Kay, L. E. (2008) Probing chemical shifts of invisible states of proteins with relaxation dispersion NMR spectroscopy: How well can we do? *J. Am. Chem. Soc.* 130, 2667–2675.

(43) Junker, J. P., and Rief, M. (2010) Evidence for a Broad Transition-States Ensemble in Calmodulin Folding from Single-Molecule Force Spectroscopy. *Angew. Chem., Int. Ed.* 49, 3306–3309.

(44) Stigler, J., Ziegler, F., Gieseke, A., Gebhardt, J. C. M., and Rief, M. (2011) The complex folding network of single calmodulin molecules. *Science* 334, 512–516.

(45) Jen, J. (1978) Chemical exchange and NMR T2 relaxation: Multisite case. *J. Magn. Reson.* 30, 111–128.

(46) Tollinger, M., Skrynnikov, N. R., Mulder, F. A. A., Forman-Kay, J. D., and Kay, L. E. (2001) Slow dynamics in folded and unfolded states of an SH3 domain. *J. Am. Chem. Soc.* 123, 11341–11352.

(47) Hill, R. B., Bracken, C., DeGrado, W. F., and Palmer, A. G. (2000) Molecular motions and protein folding: Characterization of the backbone dynamics and folding equilibrium of α D-2 using C-13 NMR spin relaxation. *J. Am. Chem. Soc.* 122, 11610–11619.

(48) Weininger, U., Liu, Z. H., McIntyre, D. D., Vogel, H. J., and Akke, M. (2012) Specific (CD2CD2SCHD2)-C-12-D- β -C-12-D- γ -C-13-H-e Isotopomer Labeling of Methionine To Characterize Protein Dynamics by H-1 and C-13 NMR Relaxation Dispersion. *J. Am. Chem. Soc.* 134, 18562–18565.

(49) Weininger, U., Blissing, A. T., Hennig, J., Ahlner, A., Liu, Z. H., Vogel, H. J., Akke, M., and Lundstrom, P. (2013) Protein conformational exchange measured by H-1 R-1 rho relaxation dispersion of methyl groups. *J. Biomol. NMR* 57, 47–55.

(50) Latham, M. P., and Kay, L. E. (2012) Is Buffer a Good Proxy for a Crowded Cell-Like Environment? A Comparative NMR Study of Calmodulin Side-Chain Dynamics in Buffer and *E. coli* Lysate. *PLoS One* 7, e48226.

(51) Ogura, K., Okamura, H., Katahira, M., Katoh, E., and Inagaki, F. (2012) Conformational dynamics of yeast calmodulin in the Ca^{2+} -bound state probed using NMR relaxation dispersion. *FEBS Lett.* 586, 2548–2554.

(52) Evenäs, J., Forsén, S., Malmendal, A., and Akke, M. (1999) Backbone dynamics and energetics of a calmodulin domain mutant exchanging between closed and open conformations. *J. Mol. Biol.* 289, 603–617.

(53) Junker, J. P., Ziegler, F., and Rief, M. (2009) Ligand-dependent equilibrium fluctuations of single calmodulin molecules. *Science* 323, 633–637.

(54) Stigler, J., and Rief, M. (2012) Calcium-dependent folding of single calmodulin molecules. *Proc. Natl. Acad. Sci. U.S.A.* 109, 17814–17819.

(55) Baldwin, R. L., Frieden, C., and Rose, G. D. (2010) Dry molten globule intermediates and the mechanism of protein unfolding. *Proteins: Struct., Funct., Bioinf.* 78, 2725–2737.

(56) Prabhu, N. V., Lee, A. L., Wand, A. J., and Sharp, K. A. (2003) Dynamics and entropy of a calmodulin-peptide complex studied by NMR and molecular dynamics. *Biochemistry* 42, 562–570.

(57) Reiner, A., Henklein, P., and Kieffhaber, T. (2010) An unlocking/relocking barrier in conformational fluctuations of villin headpiece subdomain. *Proc. Natl. Acad. Sci. U.S.A.* 107, 4955–4960.

(58) Bertini, I., Bianco, C. D., Gelis, I., Katsaros, N., Luchinat, C., Parigi, G., Peana, M., Provenzani, A., Zoroddu, M. A., and Gray, H. B. (2004) Experimentally Exploring the Conformational Space Sampled by Domain Reorientation in Calmodulin. *Proc. Natl. Acad. Sci. U.S.A.* 101, 6841–6846.

(59) Barbato, G., Ikura, M., Kay, L., Pastor, R., and Bax, A. (1992) Backbone dynamics of calmodulin studied by N-15 relaxation using inverse detected 2-dimensional NMR-spectroscopy: The central helix is flexible. *Biochemistry* 31, 5269–5278.

(60) Barton, N. P., Verma, C. S., and Caves, L. S. A. (2002) Inherent flexibility of calmodulin domains: A normal-mode analysis study. *J. Phys. Chem. B* 106, 11036–11040.

(61) Tripathi, S., and Portman, J. J. (2009) Inherent flexibility determines the transition mechanisms of the EF-hands of calmodulin. *Proc. Natl. Acad. Sci. U.S.A.* 106, 2104–2109.

(62) Wang, Q., Zhang, P., Hoffman, L., Tripathi, S., Homouz, D., Liu, Y., Waxham, M. N., and Cheung, M. S. (2013) Protein recognition and selection through conformational and mutually induced fit. *Proc. Natl. Acad. Sci. U.S.A.* 110, 20545–20550.

(63) Bayley, P. M., Findlay, W. A., and Martin, S. R. (1996) Target recognition by calmodulin: Dissecting the kinetics and affinity of interaction using short peptide sequences. *Protein Sci.* 5, 1215–1228.

(64) Hammes, G. G., Chang, Y.-C., and Oas, T. G. (2009) Conformational selection or induced fit: A flux description of reaction mechanism. *Proc. Natl. Acad. Sci. U.S.A.* 106, 13737–13741.

(65) Chattopadhyaya, R., Meador, W. E., Means, A. R., and Quiocho, F. A. (1992) Calmodulin structure refined at 1.7 Angstrom resolution. *J. Mol. Biol.* 228, 1177–1192.

(66) Meador, W. E., Means, A. R., and Quiocho, F. A. (1992) Target enzyme recognition by calmodulin: 2.4-Angstrom structure of a calmodulin-peptide complex. *Science* 257, 1251–1255.

(67) Meador, W. E., Means, A. R., and Quiocho, F. A. (1993) Modulation of calmodulin plasticity in molecular recognition on the basis of X-ray structures. *Science* 262, 1718–1721.

(68) Munz, M., Hein, J., and Biggin, P. C. (2012) The role of flexibility and conformational selection in the binding promiscuity of PDZ domains. *PLoS Comput. Biol.* 8, e1002749.

(69) Skopalik, J., Anzenbacher, P., and Otyepka, M. (2008) Flexibility of human cytochromes P450: Molecular dynamics reveals differences between CYPs 3A4, 2C9, and 2A6, which correlate with their substrate preferences. *J. Phys. Chem. B* 112, 8165–8173.

(70) Tokuriki, N., and Tawfik, D. S. (2009) Protein Dynamism and Evolvability. *Science* 324, 203–207.

(71) Shoemaker, B. A., Portman, J. J., and Wolynes, P. G. (2000) Speeding molecular recognition by using the folding funnel: The fly-casting mechanism. *Proc. Natl. Acad. Sci. U.S.A.* 97, 8868–8873.

(72) Tompa, P. (2005) The interplay between structure and function in intrinsically unstructured proteins. *FEBS Lett.* 579, 3346–3354.

(73) Uversky, V. (2009) Intrinsically disordered proteins and their environment: Effects of strong denaturants, temperature, pH, counter ions, membranes, binding partners, osmolytes, and macromolecular crowding. *Protein J.* 28, 305–325.

(74) van der Lee, R., Buljan, M., Lang, B., Weatheritt, R. J., Daughdrill, G. W., Dunker, A. K., Fuxreiter, M., Gough, J., Gsponer, J., Jones, D. T., Kim, P. M., Kriwacki, R. W., Oldfield, C. J., Pappu, R. V., Tompa, P., Uversky, V. N., Wright, P. E., and Babu, M. M. (2014) Classification of Intrinsically Disordered Regions and Proteins. *Chem. Rev.* 114, 6589–6631.

(75) Huang, Y., and Liu, Z. (2009) Kinetic Advantage of Intrinsically Disordered Proteins in Coupled Folding–Binding Process: A Critical Assessment of the “Fly-Casting” Mechanism. *J. Mol. Biol.* 393, 1143–1159.

(76) Lawrence, C. W., Kumar, S., Noid, W. G., and Showalter, S. A. (2014) Role of Ordered Proteins in the Folding-Upon-Binding of Intrinsically Disordered Proteins. *J. Phys. Chem. Lett.* 5, 833–838.